

Article

Carbon-Supported Pt-SiO₂ Catalysts for Oxygen Reduction Reaction in Low-Temperature Range: Rotating Disk Electrode Study

Ruslan M. Mensharapov ¹, Dmitry D. Spasov ^{1,2,*}, Matvey V. Sinyakov ^{1,3}, Darya E. Grineva ^{1,3},
Seraphim V. Nagorny ^{1,3}, Ratibor G. Chumakov ¹, Artem V. Bakirov ^{1,4} and Nataliya A. Ivanova ¹

¹ Department of Electrochemical and Hydrogen Technologies, National Research Center “Kurchatov Institute”, Akademika Kurchatova Sq., 1, 123182 Moscow, Russia; ruslan.mensharapov@gmail.com (R.M.M.); mmatveimatvei4@gmail.com (M.V.S.); darya19092002@gmail.com (D.E.G.); nagorny126@yandex.ru (S.V.N.); chumakov_rg@nrcki.ru (R.G.C.); bakirov.artem@gmail.com (A.V.B.); ivanovana.1989@mail.ru (N.A.I.)

² Department of Chemistry and Electrochemical Energy, National Research University “Moscow Power Engineering Institute”, Krasnokazarmennaya St., 14, 111250 Moscow, Russia

³ Department of Isotope Technology and Hydrogen Energy, Institute of Modern Energetics and Nanotechnology, D. Mendeleev University of Chemical Technology of Russia, Miusskaya Sq., 9, 125047 Moscow, Russia

⁴ Enikolopov Institute of Synthetic Polymer Materials RAS, Profsoyuznaya St., 70, 117393 Moscow, Russia

* Correspondence: spasovdd@outlook.com

Abstract: The activities of Pt electrocatalysts modified with a prepared silica powder (with SiO₂ contents of 3 and 7 wt%) in the oxygen reduction reaction in the temperature range from 0 °C to 50 °C were investigated by the rotating disk electrode technique to evaluate their efficiency in the process of the cold start of a proton-exchange membrane fuel cell (PEMFC). An increase in the mass activity of the Pt-SiO₂/C electrocatalyst in comparison with Pt/C was observed, which can be attributed to a more dispersed distribution of platinum particles on the support surface and a decrease in their size. The activity values of the silica-modified electrocatalysts in the oxygen reduction reaction were approximately two-fold higher at 1 °C and four-fold higher at elevated temperatures of up to 50 °C in comparison with Pt/C, which makes their application in PEMFCs at low temperatures, including in the process of cold start, a promising avenue for further investigation.

Keywords: PEMFC; cathode electrocatalysts; oxygen reduction reaction; rotating disk electrode; electrocatalyst activity; cold start



Academic Editor: Aleksey A. Vedyagin

Received: 8 December 2024

Revised: 14 January 2025

Accepted: 18 January 2025

Published: 21 January 2025

Citation: Mensharapov, R.M.; Spasov, D.D.; Sinyakov, M.V.; Grineva, D.E.; Nagorny, S.V.; Chumakov, R.G.; Bakirov, A.V.; Ivanova, N.A.

Carbon-Supported Pt-SiO₂ Catalysts for Oxygen Reduction Reaction in Low-Temperature Range: Rotating Disk Electrode Study. *Hydrogen* **2025**, *6*, 5. <https://doi.org/10.3390/hydrogen6010005>

Copyright: © 2025 by the authors. Licensee MDPI, Basel, Switzerland. This article is an open access article distributed under the terms and conditions of the Creative Commons Attribution (CC BY) license (<https://creativecommons.org/licenses/by/4.0/>).

1. Introduction

Environmentally friendly and renewable energy sources are being intensively introduced due to the growth of energy consumption and the efforts to reduce the emission of air pollutants and CO₂. Green hydrogen is a clean alternative to fossil fuels and, as an energy carrier in electrochemical energy systems, can be effectively used to achieve carbon neutrality [1]. The use of hydrogen fuel cells represents a comprehensive solution to the problem of energy supply in urban areas with high exhaust emissions. The utilization of power systems based on proton-exchange membrane fuel cells (PEMFCs) for vehicles represents the most promising and commercially attractive area of research and development, which is actively promoted by the governments of developed countries [2,3]. The advantages of PEMFCs, including long refueling intervals and the possibility of their effective adaptation to a wide range of environmental conditions, especially low temperatures,

make them competitive when compared with other chemical current sources, particularly lithium-ion batteries.

Recently, there has been intense growth in research on optimizing the cold-start performance of PEMFCs [4–8]. Researchers have identified a number of cold-start strategies, which can be grouped into three categories: strategies for shutdown and storage, strategies for successful start-up, and modifying the materials comprising the membrane electrode assembly (MEA) of a device [9,10]. The modification of components also appears to be a promising way to create a portable device that can be operated under nonstandard conditions, which is a common requirement for power units in transport. It is feasible to modify the membrane, and/or the catalytic layers, and/or the electrocatalyst directly as part of an MEA. The utilization of electrocatalysts as constituent elements of MEAs is a consequence of the oxygen reduction reaction (ORR) in the fuel cell cathode, which exhibits slow kinetics [11–17].

Silicon dioxide is a highly prevalent modifier in a multitude of PEMFC components [18–20], including both membranes and electrocatalysts. The incorporation of silicon dioxide into the ion channels of proton-exchange membranes as a hydrophilic material with a constant structure results in an improvement in membrane permeability due to the capillary effect [21]. Additionally, it increases membrane stiffness, which, in turn, enhances the mechanical strength of the membrane. Also, the hydrophilic nature of silica has a considerable impact on the moisture retention capacity of membranes. This is due to the enhanced retention of water in clusters, which potentially enables the utilization of such membranes in high-temperature (exceeding 120 °C) fuel cells [22–24]. Additionally, the binding of water within the clusters can impede its desorption from the membrane and prevent freezing under the influence of low temperatures.

The introduction of hydrophilic silica nanoparticles into the electrocatalyst composition significantly enhances the ability of the catalytic layer to retain water produced in the cathode [25,26]. The mechanism underlying the formation of such aqueous complexes is explained by the dissociative chemisorption of water molecules onto defects in the silicon oxide surface, followed by the physical adsorption of H₂O in multiple layers and the formation of associates with the general formula M(OH)_n(H₂O)_m [27,28]. Due to the high specific surface area of silica nanoparticle powders, their incorporation can considerably improve the water retention capacity of the electrocatalyst and the catalytic layer based on it. Keeping water bound within the volume of the cathodic catalytic layer helps prevent solidification at subzero temperatures, making it a promising strategy for enhancing the stability of the MEA during freeze–thaw cycles [29]. However, studies in which the addition of silica to the electrocatalyst structure has resulted in improved fuel cell performance during cold start are relatively limited. For electrocatalysts modified with silica, the beneficial effects of the modifier on degradation stability are more frequently assessed [30–34].

The content of modifiers in the electrocatalyst composition must also be carefully optimized. An excessive hydrophilization of the cathodic catalytic layer, resulting from high modifier concentrations at subzero temperatures, can adversely impact the degradation stability of the MEA. This instability arises from the accumulation of excess water within the layer, leading to solidification [35–40]. Moreover, an overabundance of modifiers can negatively affect the conductivity of the electrocatalyst and decrease the electrochemically active surface area of platinum, which ultimately reduces its efficiency in the ORR [21,41]. Consequently, the efficiency of cathode electrocatalysts in the ORR is critical for assessing their applicability in PEMFC applications. It is essential that these electrocatalysts exhibit high activity in a temperature range extending from 0 °C to the operating temperatures of the device [42].

Accordingly, the present study assessed the efficiency of employing modified Pt-SiO₂/C electrocatalysts for PEMFC cathode applications at low temperatures and under cold-start conditions. For this purpose, the activities of these electrocatalysts in the ORR were investigated in a temperature range of 1–50 °C.

2. Materials and Methods

In this work, electrocatalysts with Pt⁴⁰/C and Pt²⁰/SiO₂^x/C compositions (where 40, 20— wt. % of platinum; C—amorphous carbon black (Vulcan[®] XC-72, Cabot Corporation, USA); and x—3 and 7 wt. % of the silica content) were synthesized. ORISIL 300 (Polychem, Ekaterinburg, Russia) highly dispersed hydrophilic silica particles were used as a support modifier (particle size: 2–40 nm; specific surface area: 300 m² g⁻¹). The synthesis of the Pt/C electrocatalyst was carried out by the chemical reduction of H₂PtCl₆ in ethylene glycol (EG) with the preliminary sorption of the precursor onto a support. For the synthesis of the silica-modified samples, the support modification and synthesis of the SiO₂^x/C composite were carried out first. The pre-modification of the support with silica was conducted by dispersing the carbon support with prepared hydrophilic silica particles in EG and then sorbing the particles by colloid precipitation. The synthesis was then carried out similarly to the Pt/C catalyst using the methodology presented above. The detailed synthesis methodology is given in [43].

The structural study of the electrocatalysts was performed using the X-ray photoelectron spectroscopy (XPS) technique. For the XPS analysis, a PHOIBOS 150 (SPECS, Berlin, Germany) hemispherical analyzer (Al K α radiation) with a 1486.61 eV photon energy at DE = 0.2 eV was used.

This study was carried out using a three-electrode cell in a 0.1 M HClO₄ solution at atmospheric pressure. A reversible hydrogen electrode (RHE) was used as a reference electrode (a platinum electrode immersed in the electrolyte solution with a constant flow of gaseous hydrogen). The reference electrode was connected to the working electrode through a Luggin capillary. A glassy carbon disk electrode (0.102 cm²) was used as the working electrode and a platinum wire as the counter electrode. The working electrode was fixed onto the moving shaft of an RDE-06 (Volta, Saint Petersburg, Russia) capable of rotating at a predetermined speed in the speed range of 500–1600 rpm⁻¹. The specific (S_a) and mass (M_a) electrocatalyst activity were determined using Equations (1) and (2):

$$S_a = \frac{i_k}{ESA * m_{Pt}} \quad (1)$$

$$M_a = \frac{i_k}{m_{Pt}} \quad (2)$$

where m_{Pt} is the mass of Pt on the electrode, ESA is the electrochemical surface area, and i_k is the measured kinetic current. The methodology is described in more detail in [44].

3. Results and Discussion

In our previous work [43], the synthesized samples were analyzed using the following methods: Brunauer–Emmett–Teller (BET), transmission electron microscopy (TEM), energy-dispersive X-ray spectroscopy (EDX), and cyclic voltammetry. According to the results obtained, the inclusion of silicon nanoparticles in the structure of the carbon support led to an increase in the specific surface area, according to the BET method, of up to 12%. Also, smaller Pt nanoparticles were observed on the silica-modified electrocatalysts: 2.3–2.5 nm versus 2.8 nm for Pt/C. The EDX results confirmed the elemental compositions of the samples. The small size of the Pt nanoparticles on the modified samples determined higher

ESA values: $88 \text{ m}^2 \text{ g}^{-1}$, $81 \text{ m}^2 \text{ g}^{-1}$, and $42 \text{ m}^2 \text{ g}^{-1}$ for $\text{Pt}^{20}/\text{SiO}_2^3/\text{C}$, $\text{Pt}^{20}/\text{SiO}_2^7/\text{C}$, and Pt^{40}/C , respectively.

3.1. Electrocatalysts' Characterization

To further study the structures of the electrocatalysts, XPS analysis was performed. Figure 1 shows the XPS spectra in the Pt 4f, O 1s, and Si 2p regions. The spectra in the Pt 4f region demonstrate a slight downshift in the binding energies and an increase in the area of the Pt^{+2} peak for the silica-modified electrocatalysts, which can be attributed to the improved surface interaction of the platinum nanoparticles with the modified support [45,46].

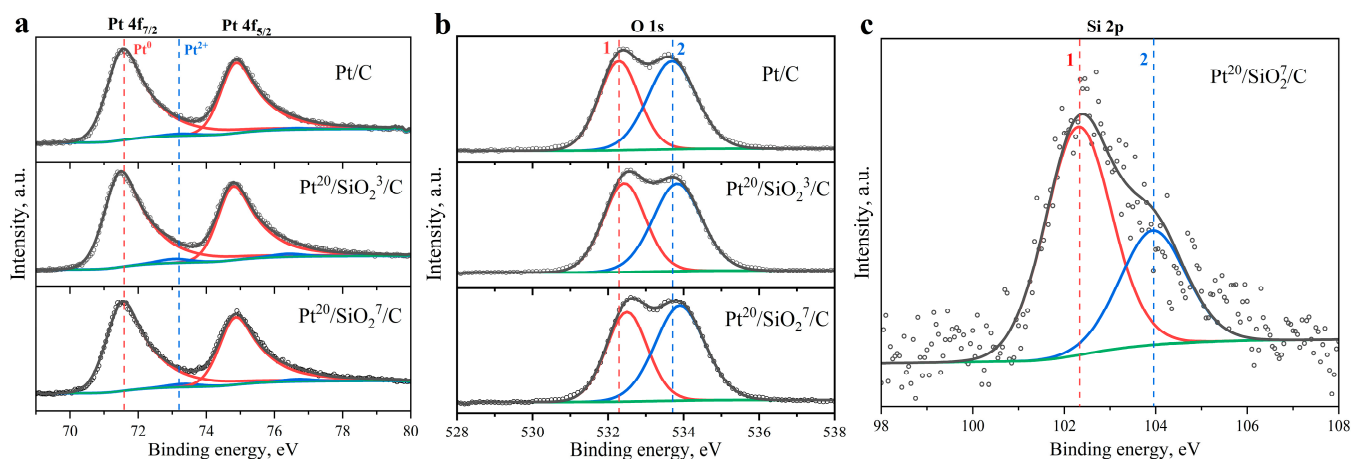


Figure 1. XPS spectral results of (a) Pt 4f, (b) O 1s, and (c) Si 2p for electrocatalyst samples. Black symbols—raw data, black line—fitted data, red and blue lines—deconvoluted peaks, green line—background.

The XPS spectra of O 1s exhibit a shift of 0.1–0.2 eV toward higher binding energies for the $\text{Pt}^{20}/\text{SiO}_2^x/\text{C}$ samples. This effect may be due to the additional contribution of a larger number of surface oxygen species caused by the incorporation of silica nanoparticles into the support [47]. The XPS results in the Si 2p region demonstrate two peaks. The peak at the higher binding energy of ~ 104 eV corresponds to SiO_2 , while the peak at the lower energy (~ 102.3 eV) can be associated with $-\text{Si}-\text{O}-\text{C}-$ and $-\text{Si}-\text{O}-\text{Pt}-$ bonds [48,49]. The higher area of the lower-energy peak confirms the involvement of a significant part of the silica surface in the interaction with the metal nanoparticles and carbon support.

3.2. Electrochemical Studies

To evaluate the effect of modifier addition on the activity of the electrocatalysts in the ORR, polarization curves were obtained by the RDE method (Figure 2).

The presented polarization curves exhibit a single pronounced wave in the region of 0.75–1.05 V vs. the RHE, as well as a stable diffusion region at a potential of less than 0.7 V vs. the RHE, which indicates the high quality of the obtained catalytic films. For all samples, the half-wave potential was observed to be in the region of 0.9 V vs. the RHE. Consequently, the activity calculations were conducted at this potential. The resulting values are presented in Table 1.

The activity values for Pt/C were found to be lower than those reported in the literature. This discrepancy can be attributed to the differences in the synthesis methods of the electrocatalysts. Nevertheless, a comparative analysis of the obtained samples was feasible.

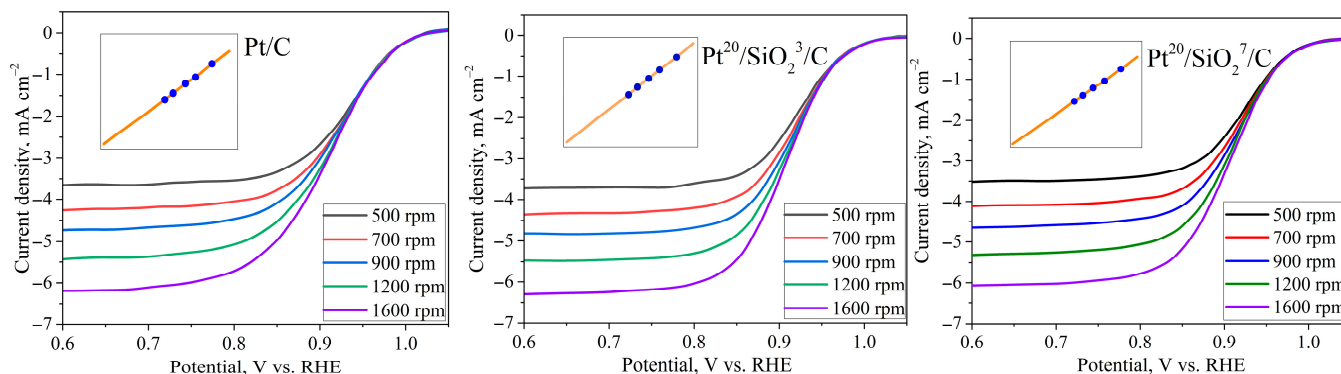


Figure 2. Polarization curves of ORR and plots in Koutecky–Levich (K–L) coordinates at 0.9 V vs. RHE.

Table 1. Kinetics parameters for ORR on Pt/C and Pt²⁰/SiO₂^x/C electrocatalysts: kinetic current density (j_k) and specific (S_a) and mass (M_a) activity at room temperature and potential at 0.9 V vs. RHE.

	j_k , mA cm ⁻²	S_a , mA cm ⁻²	M_a , mA mg ⁻¹
Pt/C	4.6 ± 0.1	0.14 ± 0.01	56 ± 1
Pt/C [50]	–	0.21	90
Pt/C [51]	–	0.19	122
Pt ²⁰ /SiO ₂ ³ /C	6.9 ± 0.3	0.25 ± 0.01	223 ± 9
Pt ²⁰ /SiO ₂ ⁷ /C	6.5 ± 0.1	0.21 ± 0.01	170 ± 3
Pt ^{46.4} /SiO ₂ ^{4.4} /C [52]	–	0.14	50
Pt ^{41.5} /SiO ₂ ⁶ /C [52]	–	0.14	60

The Pt²⁰/SiO₂^x/C samples exhibited a higher mass activity compared with the standard sample, which may be attributed to the more uniform distribution and smaller size of the Pt nanoparticles on the modified electrocatalyst. Additionally, as indicated in reference [53], the ORR activity was more pronounced in Pt with a (110) surface compared with a (100)-type surface. Furthermore, considering the previous cyclic voltammetry data [43], this effect could also have led to a higher activity value for the Pt²⁰/SiO₂³/C sample. Increasing the metal–support interaction for the modified samples may have also improved the electrocatalytic activity in the ORR [54]. An increase in the SiO₂ concentration to 7 wt% resulted in a decrease in activity. This can be attributed to the dielectric properties of the modifier, which led to an increase in the charge transfer resistance. A comparison of the results obtained in this study with previously published data for modified samples [50] revealed that the samples produced in this work exhibited approximately three to four times higher activity with a similar modifier content in their compositions (Table 1). This finding corroborates the efficiency of the sample synthesis method employed.

To evaluate the suitability of the modified electrocatalysts for cold-start applications, their ORR activities were investigated across a temperature range of 1 °C to 50 °C. Figure 3 shows the polarization curves for the Pt/C electrocatalyst at varying medium temperatures with a constant electrode rotation speed. The polarization curves demonstrate an increase in the diffusion current of the reaction with rising temperature. This phenomenon can be attributed to the slower decline in the dissolved oxygen concentration in the electrolyte in comparison with the enhanced oxygen diffusion rate to the disk electrode surface. With increasing temperature, a shift in the half-wave potential of the polarization curves toward higher potentials is also observed, which indicates a positive dependence of the reaction rate on temperature.

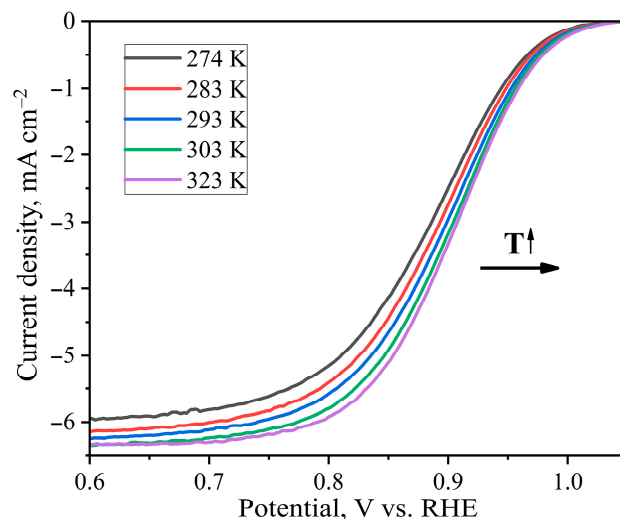


Figure 3. Polarization curves of ORR for Pt/C at an electrode rotation speed of 1600 rpm over a temperature range of 1–50 °C.

Figure 4 shows the K–L plots for the platinum electrocatalysts at 50 °C. The graphs remain parallel in the considered potential range, which indicates a weak dependence of the number of transferred electrons on the potential and the applicability of the K–L theory for elevated temperatures. The number of electrons transferred for all samples was approximately four, indicating that the electrocatalysts showed high selectivity even at elevated temperatures [44].

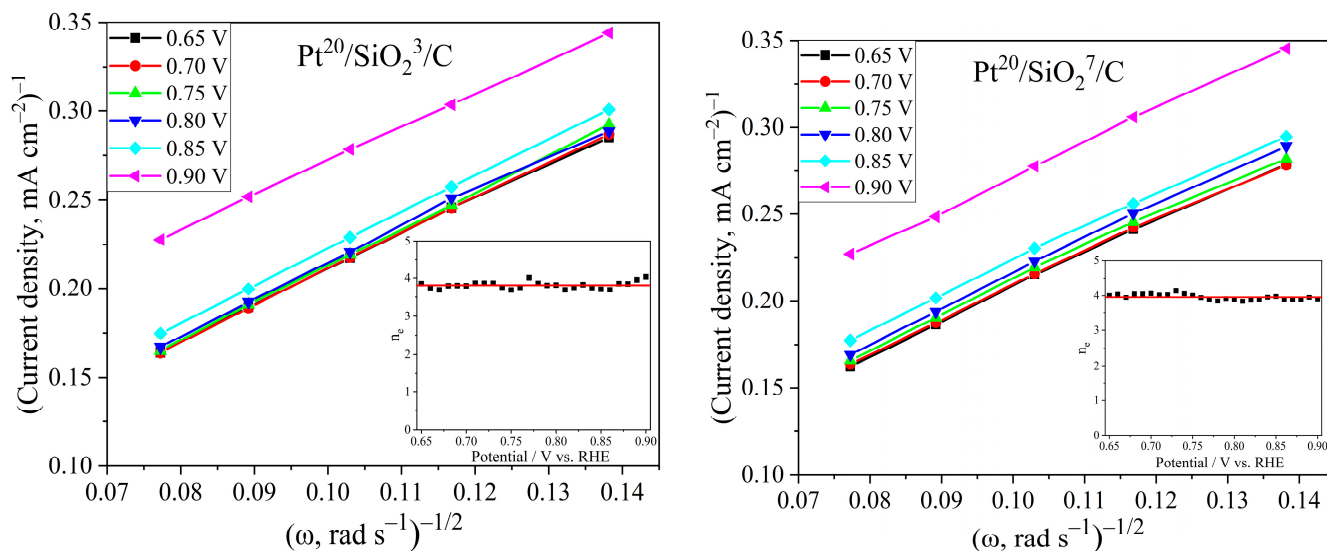


Figure 4. Graphs in K–L coordinates and the dependence of the number of transferred electrons (n_e) on the potential for the electrocatalysts in the ORR at 50 °C.

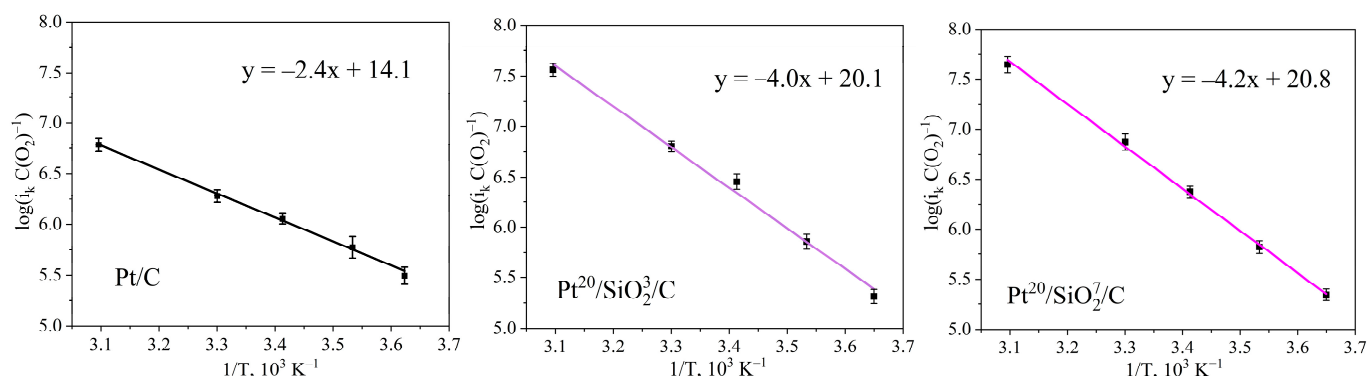
Table 2 shows the activity values in the temperature range of 1–50 °C at 0.9 V vs. the RHE.

The Pt/C electrocatalyst showed low activity values across the entire temperature range, which can be attributed to the larger size of the platinum nanoparticles and the smaller proportion of the platinum surface area involved in the ORR. Furthermore, the activity values at the different temperatures exhibited minimal variation, suggesting that the electrocatalyst efficiency was preserved at temperatures approaching 0 °C. The activity values for Pt²⁰/SiO₂^x/C were approximately twice as high as those for Pt/C at 1 °C and approximately four times higher at elevated temperatures.

Table 2. Kinetics parameters for ORR on Pt/C and Pt²⁰/SiO₂^x/C electrocatalysts in temperature range from 1 to 50 °C and at potential of 0.9 V vs. RHE.

T, K	274	283	293	303	323
Pt/C (ESA = 42 m² g⁻¹)					
<i>j_k</i> , mA cm ⁻²	3.7 ± 0.2	4.3 ± 0.3	4.6 ± 0.1	5.2 ± 0.2	5.7 ± 0.2
<i>S_a</i> , mA cm ⁻²	0.12 ± 0.01	0.13 ± 0.01	0.14 ± 0.01	0.16 ± 0.01	0.17 ± 0.01
<i>M_a</i> , mA mg ⁻¹	47 ± 2	51 ± 4	56 ± 1	62 ± 2	69 ± 2
Pt²⁰/SiO₂³/C (ESA = 88 m² g⁻¹)					
<i>j_k</i> , mA cm ⁻²	3.2 ± 0.1	4.6 ± 0.02	6.9 ± 0.27	8.7 ± 0.1	12.5 ± 0.3
<i>S_a</i> , mA cm ⁻²	0.12 ± 0.01	0.17 ± 0.01	0.25 ± 0.01	0.32 ± 0.01	0.46 ± 0.01
<i>M_a</i> , mA mg ⁻¹	104 ± 3	150 ± 5	223 ± 9	280 ± 3	402 ± 9
Pt²⁰/SiO₂⁷/C (ESA = 81 m² g⁻¹)					
<i>j_k</i> , mA cm ⁻²	3.3 ± 0.1	4.5 ± 0.1	6.4 ± 0.1	9.3 ± 0.4	13.6 ± 0.6
<i>S_a</i> , mA cm ⁻²	0.11 ± 0.01	0.15 ± 0.01	0.21 ± 0.01	0.31 ± 0.01	0.44 ± 0.02
<i>M_a</i> , mA mg ⁻¹	88 ± 2	118 ± 3	170 ± 3	248 ± 10	359 ± 16

Arrhenius plots for the studied samples are presented in Figure 5. Some plots show non-linear behavior, which may be related to the activation of additional active sites on platinum at increasing temperatures and a larger measurement error than the calculated one.

**Figure 5.** Arrhenius plots for electrocatalyst samples in ORR.

The slopes of the Arrhenius plots indicate that the activation energy (E_a) values in the ORR were 20 ± 1 , 33 ± 2 , and 35 ± 1 kJ·mol⁻¹ for Pt/C, Pt²⁰/SiO₂³/C, and Pt²⁰/SiO₂⁷/C, respectively. The obtained value of the E_a for Pt/C was in close agreement with the results presented in [55,56], where the E_a was reported to be 28 and 21 ± 3 kJ·mol⁻¹. The incorporation of SiO₂ into the electrocatalyst composition was observed to result in an increase in the energy activation by 30–40%. This phenomenon may be attributed to the partial blocking of the surfaces of platinum nanoparticles by modifier particles due to the formation of -Pt-O-Si- bonds. Nevertheless, the enhanced activity exhibited by these samples in the presented temperature range suggests that the use of such electrocatalysts in PEMFCs at low temperatures, including during the cold-start process, is a promising area for further research.

4. Conclusions

The kinetics of the oxygen reduction reaction on silica-modified electrocatalysts in a wide temperature range were investigated. The RDE method was employed to determine the kinetic and diffusion components of the ORR current. In all samples, the half-wave potential of the polarization curves was located within the region of 0.9. The RDE method

allowed for a comparative analysis of the activity values. The K–L plots at 50 °C were parallel up to the half-wave potential, indicating a weak dependence of the number of transferred electrons on the potential and the applicability of the K–L theory. Furthermore, the modified electrocatalysts displayed high selectivity for a high-temperature range. A four-fold increase in mass activity compared with the standard sample was observed for the Pt²⁰/SiO₂^x/C samples, indicating a more dispersed distribution of the platinum nanoparticles, a smaller average size, and additional platinum–support interactions. As the mass content of the modifier increased, the activity decreased by approximately 20%, which was attributed to the increased charge transfer resistance. Consequently, the activation energy for the modified electrocatalysts was observed to increase by 30–40% relative to Pt/C due to the partial blocking of the Pt surface. Nevertheless, the modified electrocatalysts exhibited a more than two-fold increase in activity at 1 °C relative to Pt/C, confirming the potential utility of silica-containing platinum electrocatalysts at low temperatures and in the cold-start process of PEMFCs.

Author Contributions: Conceptualization, R.M.M. and N.A.I.; methodology, R.M.M. and R.G.C.; software, D.D.S.; validation, A.V.B. and N.A.I.; writing—original draft preparation, R.M.M., N.A.I. and D.E.G.; writing—review and editing, D.D.S.; visualization, M.V.S. and S.V.N.; project administration, N.A.I.; funding acquisition, N.A.I. All authors have read and agreed to the published version of the manuscript.

Funding: The synthesis of the electrocatalysts was carried out within the state assignment of the NRC “Kurchatov Institute”, topic 3p.2.5. The research on the electrocatalysts was carried out within the state assignment of the NRC “Kurchatov Institute”, topic 3p.4.1.

Data Availability Statement: The data presented in this study will be made available upon request from the corresponding author.

Conflicts of Interest: The authors declare no conflicts of interest.

References

1. Yu, J.; Li, Z.; Liu, T.; Zhao, S.; Guan, D.; Chen, D.; Shao, Z.; Ni, M. Morphology Control and Electronic Tailoring of Co_xA_y (A = P, S, Se) Electrocatalysts for Water Splitting. *Chem. Eng. J.* **2023**, *460*, 141674. [[CrossRef](#)]
2. Chen, R.X.; Long, S.; He, L.; Wang, C.; Chai, F.; Kong, X.; Wan, Z.; Song, X.; Tu, Z. Performance evaluation on thermodynamics-economy-environment of PEMFC vehicle power system under dynamic condition. *Energy Convers. Manag.* **2022**, *269*, 116082. [[CrossRef](#)]
3. Bagherabadi, K.M.; Skjong, S.; Pedersen, E. Dynamic modelling of PEM fuel cell system for simulation and sizing of marine power systems. *Int. J. Hydrogen Energy* **2022**, *47*, 17699–17712. [[CrossRef](#)]
4. Voloshchenko, G.N.; Zasyapkina, A.A.; Spasov, D.D. Model Study of a Cold Start of a Power Plant Based on a Polymer Electrolyte Membrane Fuel Cells in the Conditions of Arctic Temperatures. *Nanotechnol. Russ.* **2020**, *15*, 326–332. [[CrossRef](#)]
5. Mensharapov, R.M.; Ivanova, N.A.; Spasov, D.D.; Bakirov, A.V.; Fateev, V.N. PEMFC performance at nonstandard operating conditions: A review. *Int. J. Hydrogen Energy* **2024**, *96*, 664–679. [[CrossRef](#)]
6. Lei, L.; He, P.; He, P.; Tao, W.Q. A comparative study: The effect of current loading modes on the cold start-up process of PEMFC stack. *Energy Convers. Manag.* **2022**, *251*, 114991. [[CrossRef](#)]
7. Gießgen, T.; Jahnke, T. Assisted cold start of a PEMFC with a thermochemical preheater: A numerical study. *Appl. Energy* **2023**, *331*, 120387. [[CrossRef](#)]
8. Jiang, W.; Song, K.; Zheng, B.; Xu, Y.; Fang, R. Study on Fast Cold Start-Up Method of Proton Exchange Membrane Fuel Cell Based on Electric Heating Technology. *Energies* **2020**, *13*, 4456. [[CrossRef](#)]
9. Wang, F.; Zhang, H.; Ming, P.; Yang, D.; Li, B.; Zhang, C. Experimental study on rapid cold start-up performance of PEMFC system. *Int. J. Hydrogen Energy* **2023**, *48*, 21898–21907. [[CrossRef](#)]
10. Liu, P.; Xu, S. A review of low-temperature proton exchange membrane fuel cell degradation caused by repeated freezing start. *Int. J. Hydrogen Energy* **2023**, *48*, 8216–8246. [[CrossRef](#)]
11. Zhang, J.; Yuan, Y.; Gao, L.; Zeng, G.; Li, M.; Huang, H. Stabilizing Pt-Based Electrocatalysts for Oxygen Reduction Reaction: Fundamental Understanding and Design Strategies. *Adv. Mater.* **2021**, *33*, 2006494. [[CrossRef](#)]

12. Zasyapkina, A.A.; Ivanova, N.A.; Spasov, D.D.; Mensharapov, R.M.; Sinyakov, M.V.; Grigoriev, S.A. Recent Advances in the Development of Nanocarbon-Based Electrocatalytic/Electrode Materials for Proton Exchange Membrane Fuel Cells: A Review. *Catalysts* **2024**, *14*, 303. [[CrossRef](#)]
13. Bayan, Y.; Paperzh, K.; Pankov, I.; Alekseenko, A. Influence of a carbon support on the catalytic activity and durability of the Pt-based electrocatalysts. *Mater. Lett.* **2024**, *368*, 136670. [[CrossRef](#)]
14. Paperzh, K.; Alekseenko, A.; Pankov, I.; Guterman, V. Accelerated stress tests for Pt/C electrocatalysts: An approach to understanding the degradation mechanisms. *J. Electroanal. Chem.* **2024**, *952*, 117972. [[CrossRef](#)]
15. Alekseenko, A.; Belenov, S.; Mauer, D.; Moguchikh, E.; Falina, I.; Bayan, J.; Pankov, I.; Alekseenko, D.; Guterman, V. Activity of Platinum-Based Cathode Electrocatalysts in Oxygen Redaction for Proton-Exchange Membrane Fuel Cells: Influence of the Ionomer Content. *Inorganics* **2024**, *12*, 23. [[CrossRef](#)]
16. Mensharapov, R.M.; Spasov, D.D.; Ivanova, N.A.; Zasyapkina, A.A.; Smirnov, S.A.; Grigoriev, S.A. Screening of Carbon-Supported Platinum Electrocatalysts Using Frumkin Adsorption Isotherms. *Inorganics* **2023**, *11*, 103. [[CrossRef](#)]
17. Hussain, S.; Erikson, H.; Kongi, N.; Sarapuu, A.; Solla-Gullón, J.; Maia, G.; Kannan, A.M.; Alonso-Vante, N.; Tammeveski, K. Oxygen reduction reaction on nanostructured Pt-based electrocatalysts: A review. *Int. J. Hydrogen Energy* **2020**, *45*, 31775–31797. [[CrossRef](#)]
18. Jithul, K.P.; Tamilarasi, B.; Pandey, J. Electrocatalyst for the oxygen reduction reaction (ORR): Towards an active and stable electrocatalyst for low-temperature PEM fuel cell. *Ionics* **2024**, *30*, 6757–6787. [[CrossRef](#)]
19. Xu, G.; Dong, X.; Xue, B.; Huang, J.; Wu, J.; Cai, W. Recent Approaches to Achieve High Temperature Operation of Nafion Membranes. *Energies* **2023**, *16*, 1565. [[CrossRef](#)]
20. Rodríguez-Garnica, P.; Alatorre-Ordaz, A.; Pierna, Á.R.; Guereño, M.S.; Martín, A.L. Silica based hybrid organic-inorganic materials for PEMFC application. *Int. J. Hydrogen Energy* **2020**, *45*, 16698–16707. [[CrossRef](#)]
21. Niu, J.; Zhang, S.; Li, Y.; Li, X.; Zhang, J.; Lu, S.; He, Q. Effects of microstructure on the retention of proton conductivity of Nafion/SiO₂ composite membranes at elevated temperatures: An in situ SAXS study. *Polymer* **2023**, *273*, 125869. [[CrossRef](#)]
22. Meyer, Q.; Yang, C.; Cheng, Y.; Zhao, C. Overcoming the Electrode Challenges of High-Temperature Proton Exchange Membrane Fuel Cells. *Electrochem. Energy Rev.* **2023**, *6*, 16. [[CrossRef](#)]
23. Feng, K.; Tang, B.; Wu, P. Sulfonated graphene oxide–silica for highly selective Nafion-based proton exchange membranes. *J. Mater. Chem. A* **2014**, *2*, 16083–16092. [[CrossRef](#)]
24. Liu, S.; Yu, J.; Hao, Y.; Gao, F.; Zhou, M.; Zhao, L. Impact of SiO₂ Modification on the Performance of Nafion Composite Membrane. *Int. J. Polym. Sci.* **2024**, *1*, 6309923. [[CrossRef](#)]
25. Ganesan, A.; Narayanasamy, M.; Shunmugavel, K. Self-humidifying manganese oxide-supported Pt electrocatalysts for highly-durable PEM fuel cells. *Electrochim. Acta* **2018**, *285*, 47–59. [[CrossRef](#)]
26. Amiin, I.S.; Lin, Y.; Tang, H.; Pan, M.; Zhang, H. Metal Oxides as Water Retention Materials For Low Humidity Proton Exchange Membrane Applications. *New Dev. Met. Oxides Res.* **2013**, *2*, 81–108.
27. Blesa, M.A.; Weisz, A.D.; Morando, P.J.; Salfity, J.A.; Magaz, G.E.; Regazzoni, A.E. The interaction of metal oxide surfaces with complexing agents dissolved in water. *Coord. Chem. Rev.* **2000**, *196*, 31–63. [[CrossRef](#)]
28. Leão, V.N.S.; Araújo, E.S. Metal Oxide Heteronanostructures Prepared by Electrospinning for the Humidity Detection: Fundamentals and Perspectives: 07. *J. Mater. Sci. Chem. Eng.* **2019**, *7*, 43. [[CrossRef](#)]
29. Miao, Z.; Yu, H.; Song, W.; Hao, L.; Shao, Z.; Shen, Q.; Hou, J.; Yi, B. Characteristics of proton exchange membrane fuel cells cold start with silica in cathode catalyst layers. *Int. J. Hydrogen Energy* **2010**, *35*, 5552–5557. [[CrossRef](#)]
30. Dhanasekaran, P.; Selvaganesh, S.V.; Rathishkumar, A.; Bhat, S.D. Designing self-humidified platinum anchored silica decorated carbon electrocatalyst for boosting the durability and performance of polymer electrolyte fuel cell stack. *Int. J. Hydrogen Energy* **2021**, *46*, 8143–8155. [[CrossRef](#)]
31. Dundar, F.; Uzunoglu, A.; Ata, A.; Wynne, K.J. Durability of carbon–silica supported catalysts for proton exchange membrane fuel cells. *J. Power Sources* **2012**, *202*, 184–189. [[CrossRef](#)]
32. Wu, A.; Wei, G.; Min, Y.; Huang, J.; Gao, A.; Wang, L. Enhanced cell performance: Incorporation of hydrophobic mesoporous silica into the triple-phase boundary of catalyst layer. *J. Power Sources* **2024**, *602*, 234142. [[CrossRef](#)]
33. Kong, Z.; Wu, J.; Liu, Z.; Yan, D.; Wu, Z.; Zhong, C. Advanced electrocatalysts for fuel cells: Evolution of active sites and synergistic properties of catalysts and carrier materials. *Exploration* **2023**. [[CrossRef](#)]
34. Lee, D.W.; Yuk, S.; Choi, S.; Lee, D.-H.; Doo, G.; Hyun, J.; Kwen, J.; Kim, J.Y.; Kim, H.-T. Preferential Protection of Low Coordinated Sites in Pt Nanoparticles for Enhancing Durability of Pt/C Catalyst. *Energies* **2021**, *14*, 1419. [[CrossRef](#)]
35. Seselj, N.; Alfaro, S.M.; Bompolaki, E.; Cleemann, J.N.; Torres, T.; Azizi, K. Catalyst Development for High-Temperature Polymer Electrolyte Membrane Fuel Cell (HT-PEMFC) Applications. *Adv. Mater.* **2023**, *35*, 2302207. [[CrossRef](#)]
36. Park, K.; Ohnishi, T.; Goto, M.; So, M.; Takenaka, S.; Tsuge, Y.; Inoue, G. Improvement of cell performance in catalyst layers with silica-coated Pt/carbon catalysts for polymer electrolyte fuel cells. *Int. J. Hydrogen Energy* **2020**, *45*, 1867–1877. [[CrossRef](#)]

37. Park, K.; Goto, M.; So, M.; Takenaka, S.; Tsuge, Y.; Inoue, G. Influence of Cathode Catalyst Layer with SiO₂-Coated Pt/Ketjen Black Catalysts on Performance for Polymer Electrolyte Fuel Cells. *Catalysts* **2021**, *11*, 1517. [[CrossRef](#)]
38. Zhang, R.; Chen, T.; Zhang, R.; Gan, Z. Effect of freeze–thaw cycles on membrane electrodeassembly of proton exchange membrane fuel cells and its fault diagnosis method. *Fuel Cells* **2024**, *24*, 78–89. [[CrossRef](#)]
39. Lin, R.; Zhong, D.; Lan, S.; Guo, R.; Ma, Y.; Cai, X. Experimental validation for enhancement of PEMFC cold start performance: Based on the optimization of micro porous layer. *Appl. Energy* **2021**, *300*, 117306. [[CrossRef](#)]
40. Zhang, S.; Xu, S.; Dong, F. Study on ice-melting performance of gradient gas diffusion layer in proton exchange membrane fuel cell. *Int. J. Hydrogen Energy* **2022**, *47*, 22981–22992. [[CrossRef](#)]
41. Inaba, M.; Suzuki, T.; Hatanaka, T.; Morimoto, Y. Fabrication and Cell Analysis of a Pt/SiO₂ Platinum Thin Film Electrode. *J. Electrochem. Soc.* **2015**, *162*, F634–F638. [[CrossRef](#)]
42. Sarapuu, A.; Lilloja, J.; Akula, S.; Zagal, J.H.; Specchia, S.; Tammeveski, K. Recent Advances in Non-Precious Metal Single-Atom Electrocatalysts for Oxygen Reduction Reaction in Low-Temperature Polymer-Electrolyte Fuel Cells. *ChemCatChem* **2023**, *15*, e202300849. [[CrossRef](#)]
43. Spasov, D.D.; Ivanova, N.A.; Mensharapov, R.M.; Zasyapkina, A.A.; Seregina, E.A.; Grigoriev, S.A.; Fateev, V.N. Nanostructured Pt²⁰/SiO₂^x/C Electrocatalysts for Water-Balance Stabilization in a Proton Exchange Membrane Fuel Cell. *Nanotechnol Russ.* **2022**, *17*, 320–327. [[CrossRef](#)]
44. Mensharapov, R.M.; Ivanova, N.A.; Spasov, D.D.; Kukueva, E.V.; Zasyapkina, A.A.; Seregina, E.A.; Grigoriev, S.A.; Fateev, V.N. Carbon-Supported Pt-SnO₂ Catalysts for Oxygen Reduction Reaction over a Wide Temperature Range: Rotating Disk Electrode Study. *Catalysts* **2021**, *11*, 1469. [[CrossRef](#)]
45. Spasov, D.D.; Ivanova, N.A.; Pushkarev, A.S.; Pushkareva, I.V.; Presnyakova, N.N.; Chumakov, R.G.; Presnyakov, M.Y.; Grigoriev, S.A.; Fateev, V.N. On the Influence of Composition and Structure of Carbon-Supported Pt-SnO₂ Hetero-Clusters onto Their Electrocatalytic Activity and Durability in PEMFC. *Catalysts* **2019**, *9*, 803. [[CrossRef](#)]
46. Wang, Z.; Jin, X.; Chen, F.; Kuang, X.; Min, J.; Duan, H.; Li, J.; Chen, J. Oxygen Vacancy Induced Interaction between Pt and TiO₂ to Improve the Oxygen Reduction Performance. *J. Colloid Interface Sci.* **2023**, *650*, 901–912. [[CrossRef](#)]
47. Dai, J.; Zhu, Y.; Tahini, H.A.; Lin, Q.; Chen, Y.; Guan, D.; Zhou, C.; Hu, Z.; Lin, H.-J.; Chan, T.-S.; et al. Single-Phase Perovskite Oxide with Super-Exchange Induced Atomic-Scale Synergistic Active Centers Enables Ultrafast Hydrogen Evolution. *Nat. Commun.* **2020**, *11*, 5657. [[CrossRef](#)] [[PubMed](#)]
48. Zhang, B.; Ma, P.; Wang, R.; Cao, H.; Bao, J. A Janus Platinum/Tin Oxide Heterostructure for Durable Oxygen Reduction Reaction. *Small* **2024**, *20*, 2405234. [[CrossRef](#)]
49. Katrib, A.; Stanislaus, A.; Yousef, R.M. XPS Investigations of Metal—Support Interactions in Pt/SiO₂, Ir/SiO₂ and Ir/Al₂O₃ Systems. *J. Mol. Struct.* **1985**, *129*, 151–163. [[CrossRef](#)]
50. Sun, S.; Zhang, G.; Geng, D.; Chen, Y.; Li, R.; Cai, M.; Sun, X. A Highly Durable Platinum Nanocatalyst for Proton Exchange Membrane Fuel Cells: Multiarmed Starlike Nanowire Single Crystal. *Angew. Chem.* **2011**, *123*, 442–446. [[CrossRef](#)]
51. Paperzh, K.O.; Alekseenko, A.A.; Volochaev, V.A.; Pankov, I.V.; Safronenko, O.A.; Guterman, V.E. Stability and Activity of Platinum Nanoparticles in the Oxygen Electroreduction Reaction: Is Size or Uniformity of Primary Importance? *Beilstein J. Nanotechnol.* **2021**, *12*, 593–606. [[CrossRef](#)] [[PubMed](#)]
52. Pinchuk, O.A.; Dunder, F.; Ata, A.; Wynne, K.J. Improved Thermal Stability, Properties, and Electrocatalytic Activity of Sol-Gel Silica Modified Carbon Supported Pt Catalysts. *Int. J. Hydrogen Energy* **2012**, *37*, 2111–2120. [[CrossRef](#)]
53. Markovic, N.; Gasteiger, H.; Ross, P.N. Kinetics of Oxygen Reduction on Pt (Hkl) Electrodes: Implications for the Crystallite Size Effect with Supported Pt Electrocatalysts. *J. Electrochem. Soc.* **1997**, *144*, 1591. [[CrossRef](#)]
54. Esfahani, R.A.M.; Moghaddam, R.B.; Ebraliidze, I.I.; Easton, E.B. A Hydrothermal Approach to Access Active and Durable Sulfonated Silica-Ceramic Carbon Electrodes for PEM Fuel Cell Applications. *Appl. Catal. B Environ.* **2018**, *239*, 125–132. [[CrossRef](#)]
55. Jäger, R.; Härk, E.; Steinberg, V.; Lust, E. Influence of Temperature on the Oxygen Electroreduction Activity at Nanoporous Carbon Support. *ECS Trans.* **2015**, *66*, 47. [[CrossRef](#)]
56. Paulus, U.A.; Schmidt, T.J.; Gasteiger, H.A.; Behm, R.J. Oxygen reduction on a high-surface area Pt/Vulcan carbon catalyst: A thin-film rotating ring-disk electrode study. *J. Electroanal. Chem.* **2001**, *495*, 134–145. [[CrossRef](#)]

Disclaimer/Publisher’s Note: The statements, opinions and data contained in all publications are solely those of the individual author(s) and contributor(s) and not of MDPI and/or the editor(s). MDPI and/or the editor(s) disclaim responsibility for any injury to people or property resulting from any ideas, methods, instructions or products referred to in the content.